## Original Article
# Effects of microRNA-29a on retinopathy of prematurity by targeting AGT in a mouse model

Xin-Ke Chen[1], Li-Juan Ouyang[1], Zheng-Qin Yin[2], Yuan-You Xia[1], Xiu-Rong Chen[1], Hui Shi[1], Yan Xiong[1], Lian-Hong Pi[1]

[1]Department of Ophthalmology, Children's Hospital of Chongqing Medical University, Chongqing 400014, P. R. China; [2]Department of Ophthalmology, Southwest Hospital, Third Military Medical University, Chongqing 400038, P. R. China

**Abstract:** Background: This study aimed to explore the effects of microRNA-29a (miR-29a) on retinopathy of prematurity (ROP) by targeting angiotensinogen (AGT) expression in a mouse model. Methods: Ninety-six C57BL/6J mice were selected and divided into the normal control group (n = 12) and the oxygen-induced retinopathy (OIR) group (n = 84). All the mice in the OIR group were assigned to the following seven groups (12 mice in each group): the blank, miR-29a mimics, miR-29a inhibitors, empty plasmid, miR-29a mimics + si-AGT, miR-29a inhibitors + si-AGT and si-AGT groups. ADPase histochemical staining was conducted to detect the morphology of retinal neovascularization. H&E staining was performed to quantify retinal neovascularization. The qRT-PCR assay was applied to detect the expression levels of miR-29a and the *AGT* mRNA. Western blotting was used to detect the protein expressions of AGT, vascular endothelial growth factor (VEGF), hepatocyte growth factor (HGF), angiotensin (ANG) and angiotensin II (AngII). Results: Compared with the normal control group, miR-29a expression decreased, while the *AGT* mRNA expression and the protein expression levels of AGT, VEGF, HGF, ANG and AngII increased, and retinal vascular density and neovascularization also increased in the OIR group. In the OIR group, compared with the blank, empty plasmid, miR-29a inhibitors and miR-29a inhibitors + si-AGT groups, miR-29a expression increased, while the *AGT* mRNA expression and protein expression levels of AGT, VEGF, HGF, ANG and AngII decreased, and retinal vascular density and neovascularization also decreased in the miR-29a mimics, miR-29a mimics + si-AGT and si-AGT groups. Conclusion: MiR-29a could inhibit retinal neovascularization to prevent the development and progression of ROP by down-regulating AGT.

**Keywords:** miRNA-29a, AGT, retinopathy of prematurity, mouse model

## Introduction

Retinopathy of prematurity (ROP) is a proliferative disease of retinal vascular tissues in premature and low birth weight infants [1]. In 2010, approximately 20,000 infants worldwide became severely visually impaired or blind because of ROP [2]. The development of ROP is affected by many factors, including low birth weight, infection, gestational age at birth, and the duration and intensity of post-natal supplemental oxygen therapy [1, 3, 4]. The pathogenesis of ROP is not yet entirely clear, and factors such as vascular endothelial growth factor (VEGF), matrix metalloproteinase (MMP), and pigment epithelium-derived factor (PEDF) might be involved [5-7]. The treatments for ROP

include cryotherapy and laser therapy, and novel targeted therapies are currently popular research topics [8-10].

It was shown that microRNAs (miRs), such as miR-31, miR-205, miR-488 and miR-20b, changed their expression levels in animal models of retinal diseases [11]. MiR-29 is an important family that includes miR-29a, miR-29b and miR-29c [12]. MiR-29a might be related to angiogenesis and fibrosis in the vitreous of eyes with proliferative diabetic retinopathy (PDR) [13]. The human AGTgene codes for the expression of angiotensinogen (AGT) protein, which is an abundant glycoprotein in serum [14, 15]. AGT is a major component of the renin-angiotensin system (RAS), and angiotensin II (AngII) is

**Table 1.** Oligonucleotide sequences of RNA and DNA

| Name | Sequence |
|------|----------|
| Mus-miR-29a mimic | 5'-TAACCGATTTCAGATGGTGCTA-3' |
| Mus-miR-29a inhibitor | 5'-UAACCGAUUUCAGAUGGUGCUA-3' |
| si-AGT | 5'-GGCCACCATCTTCTGCATC-3' |
| NC | 5'-UUCUCCGAACGUGUCACGUdTdT-3' |
| AGT | Upstream: 5'-GCCTCGAGAAGATGAGAGGCTTCTCCCA-3' |
| | Downstream: 5'-GCAAGCTTTCCACTCTGCCCAGAAAGT-3' |
| GAPDH | Upstream: 5'-CTGCACCACCAACTGCTTAG-3' |
| | Downstream: 5'-TGAAGTCAGAGGAGACCACC-3' |

Notes: NC = negative control; GAPDH = glyceraldehyde phosphate dehydrogenase; AGT = angiotensinogen.

the end product of the RAS [16]. AngII has been found to regulate blood pressure and to promote atherosclerosis [17]. In the occurrence and development of proliferative retinopathy, AngII interacts with specific growth factors, such as VEGF, to influence retinal angiogenesis, eventually leading to retinal neovascularization [18, 19]. Wu et al. demonstrated that the efficiency of AGT cleavage determined the rate of AngII production and consequently influenced AngII-mediated physiological and pathophysiological effects [17]. With the above information considered, we conducted the current study to clarify the roles of miR-29a and its targeted gene AGT in an ROP mouse model with the aims of exploring the pathogenesis of ROP and of investigating the potential role of miR-29a in treating ROP.

## Materials and methods

### Ethical statement

The animal experiments were designed with the consent of the animal ethics committee, and all the studies were conducted strictly in accordance with international standards.

### Establishment of a ROP mouse model

A total of 96 newborn C57BL/6J mice were purchased from the Department of Experimental Animals of Chongqing Medical University. All the mice were assigned to the normal control group (n = 12) and the OIR group (n = 84). On postnatal day 7 (P7), the mice in the OIR group were incubated in an oxygen tank (75 ± 2% oxygen) for 5 days and were returned to a normal air environment on day P12 for different treatments [20]. In the normal control group, the

mice had free access to water, food and natural light. On day P17, hematoxylin and eosin (HE) staining of retinal tissue sections and adenosine diphosphatase (ADPase) staining of retinal stretched preparations were conducted.

### Construction of plasmid vectors

The miR-29a mimics were synthesized based on the mature sequence (accession No. MI0000576, miRBase). A reverse complementary sequence of mature miR-29a was used as the miR-29a inhibitor. AGT silencing was conducted based on the design principles of si-RNA and was verified through homology analysis. The negative control (NC) of the double-stranded RNA is a random sequence with no homology in the mammalian genome. During the synthesis of the oligonucleotides (Genepharma, Shanghai, China), BAM HI and Xho I restriction enzyme cutting sites were added at both ends of the synthetic sequence (**Table 1**). The sequence fragments were cloned into the pRNA-Lenti-EGFP lentiviral vector to generate corresponding transfection plasmids as follows: pRNA-Lenti-miR-29a mimic-EGFP plasmid (miR-29a mimics plasmid), pRNA-Lenti-miR-29a inhibitor-EGFP plasmid (miR-29a inhibitors plasmid), pRNA-Lenti-si-AGT-EGFP plasmid (AGT silencing plasmid) and pRNA-Lenti-vector-EGFP plasmid (empty plasmid). At the same time, the fragments of the AGT target gene was inserted into the wild-type AGT-3'UTR-WT and mutant-type AGT-3'UTR-MUT plasmids to construct a dual-luciferase reporter gene plasmid.

### Dual-luciferase reporter gene assay

Bioinformatics software (http://www.target-scan.org) was used to predict the targeting relationship between miR-29a and AGT and the binding sites of miR-29a and AGT 3'UTR. The AGT 3'UTR promoter region sequence containing the miR-29a binding site was synthesized and inserted into the 5' end BglII binding site of the pGL3 control vector (Promega Corporation,

Madison, WI, USA) to construct the AGT 3'UTR wild-type plasmid (AGT 3'UTR-WT). The AGT 3'UTR mutant type plasmid (AGT 3'UTR-MUT) was constructed based on AGT 3'UTR-WT with the mutant binding site of miR-29a. The construction of plasmids was performed with a plasmid isolation kit (Promega Corporation, Madison, WI, USA). In the dual-luciferase reporter gene assay, 293T cells in logarithmic growth were seeded in 96-well plates and were cultured to approximately 70% confluency, and then they were co-transfected with AGT-3'UTR-WT plasmids and miR-29a mimics plasmidsusing Lipofectamine 2000 (AGT 3'UTR-WT + miR-29a mimics). AGT 3'UTR-WT +_NC, AGT 3'UTR-MUT + NC and AGT 3'UTR-MUT + miR-29a mimics were transfected into 293T cells as the control groups. After culture in an incubator for 6 h, the cells were cultured in the medium containing 10% FBS for 48 h. Then, luciferase activity was detected by chemiluminescence assay.

*Cell transfection and grouping*

The 293T cells in logarithmic growth (Shanghai Cell Bank, Shanghai, China) were seeded into 96-well plates (100 µl/well) and were transfected with corresponding plasmids and lentiviral packaging. At 24 h after transfection, 293T cells containing miR-29a mimics plasmids, miR-29a inhibitors plasmids, si-AGT plasmids and empty plasmids were collected. Then, the cells were seeded into 96-well plates using dilution factors of $10^{-4}$, $10^{-5}$, $10^{-6}$, $10^{-7}$ and $10^{-8}$, each with 3 duplicate wells. The cells were cultured for additional 18 h at 37°C with 5% $CO_2$ and were counted under an inverted fluorescence microscope (Nikon, Japan) to calculatethe virus titer (pfu/ml), which refers to (10 × the average fluorescence intensity)/corresponding dilution factors. The cells were collected after 48 h. The total RNA was isolated using an RNA isolation kit (Invitrogen Inc., Carlsbad, CA, USA). The expression levels of miR-29a and AGT mRNA were detected by quantitative real-time polymerase chain reaction (qRT-PCR).

Ninety-six mice were assigned to the normal control group (without any treatment), the OIR group, the blank group (OIR mice without any treatment), the miR-29a mimics group (OIR mice with intravitreal injection of 4 µg miR-29a mimic plasmids), the miR-29a inhibitors group (OIR mice with intravitreal injection of 4 µg miR-29a inhibitor plasmids), the empty plasmid group (OIR mice with intravitreal injection of 4 µg empty plasmids), the miR-29a mimics + si-AGT group (OIR mice with intravitreal injection of 4 µg miR-29a mimic plasmids and 4 µg si-AGT plasmids), the miR-29a inhibitors + si-AGT group (OIR mice with intravitreal injection of 4 µg miR-29a inhibitor plasmids and 4 µg si-AGT plasmids) and the si-AGT group (OIR mice with intravitreal injection of 4 µg si-AGT plasmids). Each group had 12 mice.

*Adenosine diphosphatase (ADPase) histochemical staining*

The mice were sacrificed by intraperitoneal injection of 3% pentobarbital (2 ml/kg) under anesthesia. The eyes were enucleated and soaked in 10% formalin for 12 h. Then, the lens, cornea, choroid and sclera were removed under a dissecting microscope. After the removal of the vitreous body and retinal pigment epithelium, free retinas were obtained and divided into 4 symmetric quadrants centered on the optic disk. The samples were washed with purified water for 12 h and were digested with 3% trypsin at 37°C for 7 h. Then, ADPase histochemical staining was conducted. The samples were rinsed 5 times (15 min each time) with pre-cooled 50 mM Tris-maleic acid buffer. Subsequently, the samples were soaked in 0.2 mM Tris-maleic acid buffer containing 1 mg/ml ADP at 37°C for 15 min and were rinsed 5 times again (15 min each time) with 50 mM Tris-maleic acid buffer. The stained samples were developed in 1:10 ammonium sulfide for 10 min and were rinsed 3 times (15 min each time) with 50 mM Tris-maleic acid buffer. The samples were mounted in 50% glycerol, observed under an optical microscope and photographed using a digital camera.

*HE staining*

The mouse retinal tissues were collected. After fixation in Davidson's solution for 24 h, the samples underwent routine dehydration, transparent, paraffin impregnation and paraffin embedding. Ten serial sections with a thickness of 3 µm were baked at 50°C for 1 h. The samples were stained with HE. The extent of retinal angiogenesis was observed under a microscope. A double-blind method was used to determine the amount of retinal neovascularization and to calculate the average.

**Table 2.** qRT-PCR primer sequences

| Gene | Sequences |
|------|-----------|
| miRNA-29a | Upstream: 5'-CTGATTTCTTTTGGTGTTCA-3' |
| | Downstream: 5'-TGGTGTCGTGGAGTCG-3' |
| AGT | Upstream: 5'-GCCTCGAGAAGATGAGAGGCTTCTCCCA-3' |
| | Downstream: 5'-GCAAGCTTTCCACTCTGCCCAGAAAGT-3' |
| GAPDH | Upstream: 5'-CTGCACCACCAACTGCTTAG-3' |
| | Downstream: 5'-TGAAGTCAGAGGAGACCACC-3' |

Notes: GAPDH = glyceraldehyde phosphate dehydrogenase; qRT-PCR = quantitative real-time polymerase chain reaction; AGT = angiotensinogen.

*Quantitative real-time polymerase chain reaction (qRT-PCR)*

The mouse retinal tissues were ground in normal saline. The total RNA of transfected cells and mouse retinal tissues was isolated using an RNA isolation kit (Invitrogen Inc., Carlsbad, CA, USA). The primers for miR-29a, AGT mRNA and *GAPDH* mRNA were synthesized by TaKaRa (**Table 2**). The total RNA was reversely transcribed to cDNA using a PrimeScript RT reagent Kit (TaKaRa Holdings Inc., Kyoto, Japan). The reverse transcription system was 10 µl. The reaction conditions were a reverse transcription reaction at 37°C for 15 min in triplicate and a reverse transcription inactivation reaction at 85°C for 5 s. The qRT-PCR reaction was conducted using a Premix Ex TaqII SYBR kit (TaKaRa Holdings Inc., Kyoto, Japan). The reaction conditions were pre-denaturation at 95°C for 15 min, denaturation at 95°C for 15 s, and annealing and extension at 60°C for 60 s (40 cycles). The reaction system included 2 µl of upstream primer, 2 µl of downstream primer, 4 µl of DNA template, 1 µl of ROX Reference Dye (50 ×), 25 µl of SYBR Premix Ex TaqII, and 16 µl of dH$_2$O. GAPDH was used as the internal control. The expression levels of miR-29a and AGT mRNA were calculated via the $2^{-\Delta\Delta Ct}$ method, where Ct is the cycle threshold value.

*Western blotting*

After grinding in normal saline, the mouse retinal tissues were centrifuged at 12,000 rpm for 15 min, and the supernatant was collected. The protein content in the supernatant was measured by the BCA method. For antibody staining experiments, the samples underwent sodium dodecyl sulfate-polyacrylamide gel electrophoresis (SDS-PAGE) and were transferred onto a nitrocellulose membrane. The membrane was blocked with 5% skim milk for 1.5 h and was incubated overnight at 4°C with primary antibodies (1:500 dilution, PL Laboratories, British Columbia, Canada), including AGT (PL0301407), VEGF (PL0305639), HGF (PL0303330) and ANG (PL0300688) and AngII (PL0301232). Subsequently, the membrane was washed with PBST 5 times and was incubated with horseradish peroxidase-labeled IgG secondary antibodies (Cell Signal Technology, USA) for 2 h. After washing with PBST at least 3 times, the membrane was exposed to ECL reagent and was photographed with a gel imaging system (Bio-Rad, Inc., Hercules, CA, USA). Then, the gray values of the bands were analyzed, with GAPDH (Bioworld, USA) as the internal control. The relative protein expression was calculated as the ratio of the gray value of the target band to that of the internal control band.

*Statistical analysis*

Data were analyzed with SPSS software, version 21.0 (SPSS Inc.; Chicago, IL, USA). The continuous data are presented as the mean ± standard deviation ($\overline{x}$ ± s). The *t*-test was applied for pairwise comparisons. One-way analysis of variance (ANOVA) was used for multi-group comparisons. The $x^2$ test was used for comparisons among categorical data. *P*<0.05 was considered to indicate statistical significance.

**Results**

*Successful establishment of OIR mouse models*

The survival rate of the mice was 100% during the experiments. Before modeling, there was no significant difference in retinal neovascularization between the normal control and OIR groups (*P*>0.05). On day P12 after modeling, in the normal control group, the retinal vessels in the mice showed a radial pattern with adequate caliber and good branches, and the two layers of the vascular network could be easily distinguished (**Figure 1A**). In the OIR group, the central retinal vessels were thinner with fewer branches, and a nonperfusion area could be seen around the central retina (**Figure 1B**). On day P14, in the normal control group, the retinal
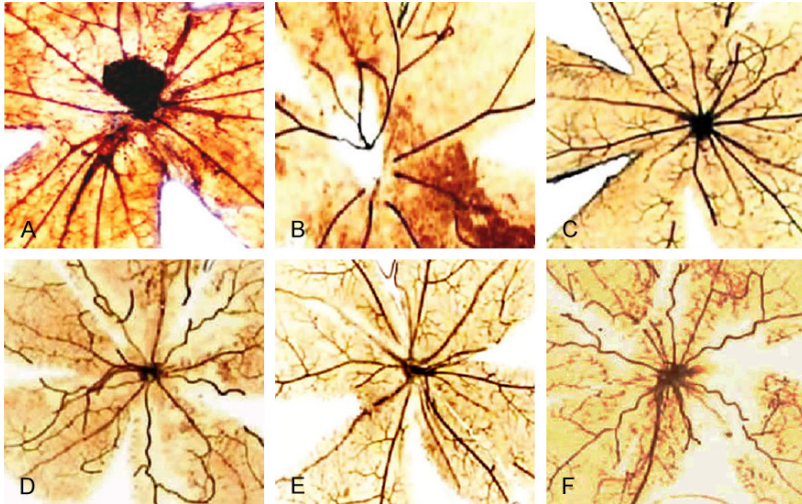
**Figure 1.** ADPase staining (× 200) of the retinal stretched preparations. Notes: A. Air group on day P12; B. High oxygen group on day P12; C. Air group on day P14; D. High oxygen group on day P14; E. Air group on day P17; F. High oxygen group on day P17. ADPase = adenosine diphosphatase.
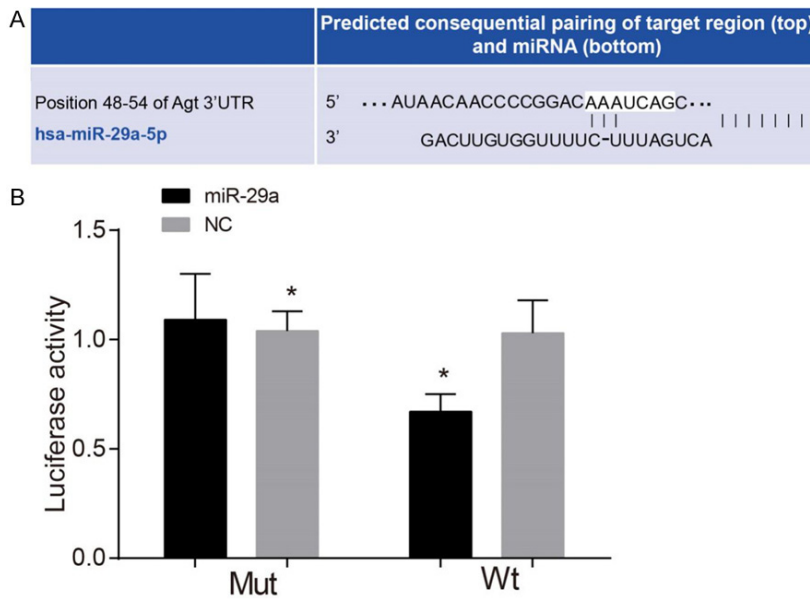


**Figure 2.** Verification of the targeting relationship between miR-29a and AGT. Notes: A. The binding site of miR-29a and AGT 3'UTR; B. The luciferase expression of 293T cells at 48 h after transfection using AGT-3'UTR-WT + miR-29a mimic/NC and AGT-3'UTR-MUT + miR-29a mimic/NC plasmids; *refers to *P*<0.05; NC = negative control; AGT = angiotensinogen.

fully reached maturity, and the two layers of the vascular network were connected to each other (**Figure 1E**). In the OIR group, retinal dilation and tortuosity became more apparent, and the nonperfusion area decreased (**Figure 1F**). The results indicated that the oxygen-induced retinal neovascularization in the mouse model was successfully constructed.

*AGT as a direct target gene of miR-29a*

The results from the bioinformatics software (http://www.targetscan.org) predicted that miR-29a and AGT had a targeting relationship (**Figure 2A**). The 293T cells were co-transfected with AGT-3'UTR-WT and miR-29a mimics plasmids. The statistical analysis indicated that the luciferase activity decreased in the AGT-3'UTR-WT + miR-29a mimics group, compared with the AGT-3'UTR-WT + NC group (*P*<0.05). The luciferase activity exhibited no significant difference between the AGT-3'UTR-MUT + NC and AGT-3'UTR-MUT + miR-29a mimics groups (*P*>0.05) (**Figure 2B**).

*Transfection efficacy of miR-29a and si-AGT*

The rpRNA-Lenti-miR-29a mimic-EGFP (miR-29a mimics plasmids), pRNA-Lenti-miR-29a inhibitor-EGFP (miR-29a inhibitors plasmids), pRNA-Lenti-si-AGT-EGFP (AGT silencing plasmids) and pRNA-Lenti-vector-EGFP (empty plasmids) were transfected into 293T cells. The expression of green fluorescent protein (GFP) was observed under a fluorescence microscope. The results

vessels nearly reached maturity with a uniform distribution (**Figure 1C**). In the OIR group, retinal vascular dilation and tortuosity were observed, a nonperfusion area could be seen in the central retina, and the density of peripheral vessels increased (**Figure 1D**). On day P17 in the normal control group, the retinal vessels
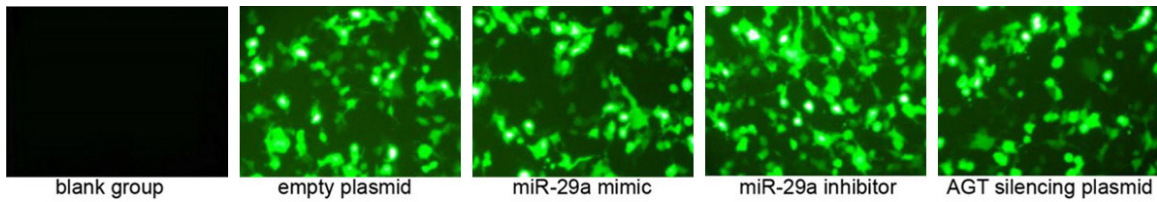
Figure 3. Fluorescence images of 293T cells infected by recombinant virus (× 100).

Table 3. Comparisons of vascular density and the number of retinal neovascularization in eight groups

| Group | Vascular density | Neovascularization |
|---|---|---|
| Normal control group | 20.83 ± 3.49 | 3.50 ± 0.52 |
| Blank group | 47.67 ± 4.38[a] | 22.92 ± 3.53[a] |
| MiR-29a mimics group | 33.67 ± 3.31[b] | 16.25 ± 1.91[b] |
| MiR-29a inhibitors group | 60.00 ± 6.54[d] | 48.83 ± 5.22[d] |
| Empty plasmid group | 45.67 ± 4.38[a] | 22.00 ± 4.09[a] |
| MiR-29a mimics + si-AGT group | 26.00 ± 2.26[c] | 9.17 ± 2.44[c] |
| MiR-29a inhibitors + si-AGT group | 42.92 ± 3.29[a] | 23.17 ± 3.81[a] |
| si-AGT group | 32.92 ± 2.31[b] | 17.17 ± 1.99[b] |

Notes: lowercase letters (a, b, c and d) indicate P<0.05 compared with the normal control group: different letters indicate P<0.05 compared between two groups, while the same letters indicate P>0.05 compared between two groups.

showed that the cells in 4 groups were green-emitting, indicating successful transfection (**Figure 3**). After multiple rounds of transfection, the titer reached $10^8$ pfu/ml.

*Morphology of retinal neovascularization*

ADPase histochemical assay was used to detect the morphology of retinal neovascularization. In the normal control group, the retinal vessels showed a straight-line pattern with good branches and a visible two-layer structure. In addition, the vessels emanated evenly from the optic disc to the surroundings, and the peripheral retinal vessels could be clearly seen. Compared with the normal control group, the retinal vessels showed vascular derangements and tortuosity, and retinal vascular density was increased significantly in the OIR group (all P<0.05). There were no significant differences among the blank, empty plasmid and miR-29a inhibitors + si-AGT groups, nor were there any differences between the miR-29a mimics and si-AGT groups (all P>0.05). Compared with the blank, empty plasmid and miR-29a inhibitors + si-AGT groups, the vascular density and the tortuosity significantly decreased in the miR-29a mimics, miR-29a mimics + si-AGT and si-AGT groups (all P<0.05). The vascular density and the tortuosity in the miR-29a mimics + si-AGT group were lower than those in the miR-29a mimics group. The vascular density and tortuosity in the miR-29a inhibitors group were higher than those in the miR-29a inhibitors + si-AGT group (both P<0.05) (**Table 3**).

HE staining was conducted to determine the amount of retinal neovascularization. In the normal control group, the internal limiting membrane in tissue sections was clear and continuous, and neovascularization in the vitreous body near the retinal inner limiting membrane was seen only in a few sections. In the OIR group, the internal limiting membrane was not continuous, and a small amount of neovascularization was seen in the vitreous body. There were no significant differences among the blank, empty plasmid, and miR-29a inhibitors + si-AGT groups, nor were there any differences between the miR-29a mimics and si-AGT groups (all P>0.05). Compared with the blank, empty plasmid and miR-29a inhibitors + si-AGT groups, the amount of neovascularization was significantly decreased in the miR-29a mimics, miR-29a mimics + si-AGT and si-AGT groups (all P<0.05). The amount of neovascularization in the miR-29a mimics + si-AGT group was lower than that in the miR-29a mimics group. The amount of neovascularization in the miR-29a inhibitors group was higher than that in the miR-29a inhibitors + si-AGT group (all P<0.05) (**Table 3**; **Figure 4**). These results indicated that miR-29a mimics/inhibitors could inhibit/promote the occurrence of retinopathy. In addition, these effects could be reversed by silencing AGT.

*Expression levels of miR-29a and AGT mRNA in 293T cells*

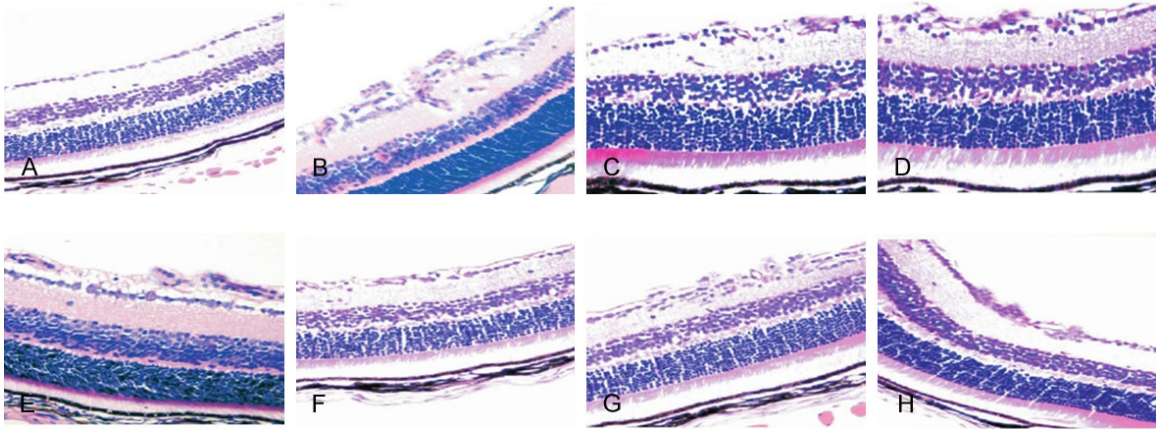Expression levels of miR-29a and AGT mRNA in 293T cells were measured by qRT-PCR assay.

**Figure 4.** HE staining of retinal neovascularization in eight groups (× 200). Notes: A. Normal control group; B. Blank group; C. miR-29a mimics group; D. miR-29a inhibitors group; E. Empty plasmid group; F. miR-29a mimics + si-AGT group; G. miR-29a inhibitors + si-AGT group; H. si-AGT group; HE = hematoxylin and eosin; AGT = angiotensinogen.
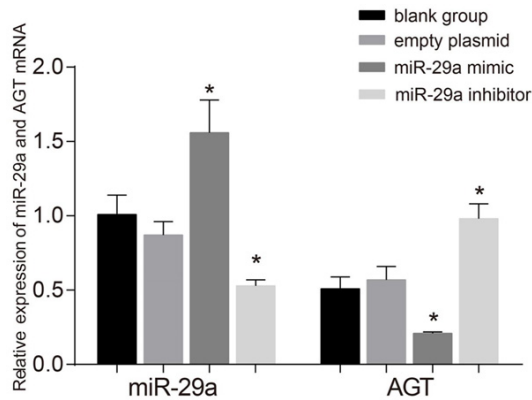


**Figure 5.** The miR-29a and *AGT* mRNA expression levels after transfection for 48 h in 293T cells. Notes: *refers to *P*<0.05, compared with the blank group; AGT = angiotensinogen.



**Figure 6.** The expressions of miR-29a and *AGT* mRNA in eight groups. Notes: A. normal control group; B. blank group; C. miR-29a mimics group; D. miR-29a inhibitors group; E. empty plasmid group; F. miR-29a mimics + si-AGT group; G. miR-29a inhibitors + si-AGT group; H. si-AGT group; lowercase letters indicate *P*<0.05, compared with the normal control group: different letters indicate *P*<0.05 comparing two groups, while the same letters indicate *P*>0.05 comparing two groups; AGT = angiotensinogen.

There were no significant differences between the blank group and the empty plasmid group (*P*>0.05). Compared with the blank and empty plasmid groups, the miR-29a expression significantly increased, and the AGT mRNA expression significantly decreased in the miR-29a mimics group, while the miR-29a expression significantly decreased, and the AGT mRNA expression significantly increased in the miR-29a inhibitors group (all *P*<0.05) (**Figure 5**).

*Correlations of miR-29a and AGT with ROP*

Compared with the normal control group, the miR-29a expression significantly decreased, while the mRNA and protein expression levels
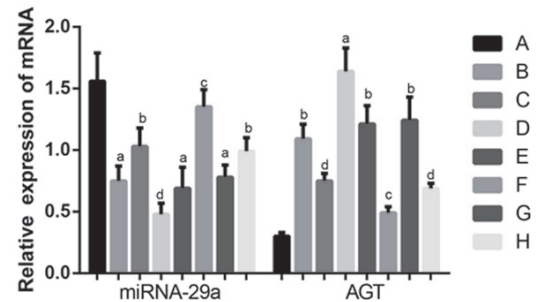
of AGT significantly increased in the OIR group (all *P*<0.05). There were no significant differences among the blank, empty plasmid, and miR-29a inhibitors + si-AGT groups, nor were there any differences between the miR-29a mimics and si-AGT groups. Compared with the blank, empty plasmid and miR-29a inhibitors + si-AGT groups, the miR-29a expression significantly increased, while the mRNA and protein expression levels of AGT significantly decreased in the miR-29a mimics, miR-29a mimics + si-AGT and si-AGT groups. The miR-29a expression significantly decreased, while the mRNA and protein expression levels of AGT signifi-
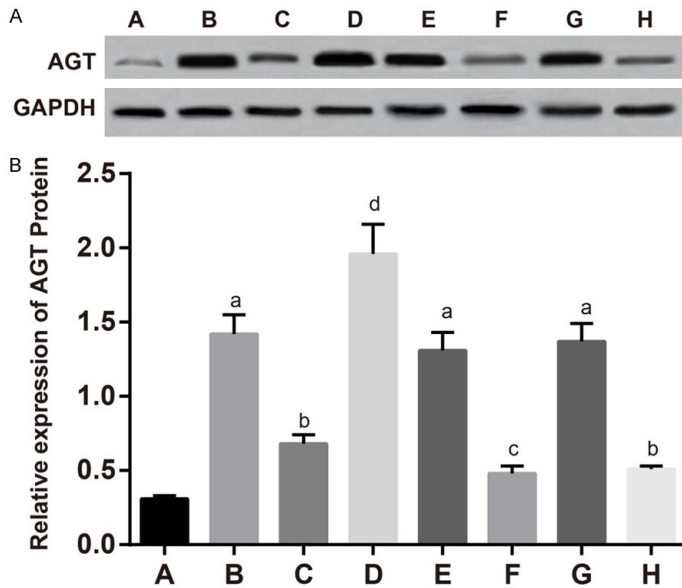
**Figure 7.** The AGT protein expression in eight groups. Notes: A. normal control group; B. blank group; C. miR-29a mimics group; D. miR-29a inhibitors group; E. empty plasmid group; F. miR-29a mimics + si-AGT group; G. miR-29a inhibitors + si-AGT group; H. si-AGT group; lowercase letters indicate $P<0.05$ compared with the normal control group, different letters indicate $P<0.05$ comparing two groups, and the same letters indicate $P>0.05$ comparing two groups; AGT = angiotensinogen.

cantly increased in the miR-29a inhibitors group (**Figures 6**, **7**).

*Comparisons of the protein expression levels of VEGF, HGF, ANG and AngII among the eight groups*

Compared with the normal control group, the expression levels of VEGF, HGF, ANG and AngII significantly increased in the OIR group (all $P<0.05$). There were no significant differences among the blank, empty plasmid, and miR-29a inhibitors + si-AGT groups, nor were there any differences between the miR-29a mimics and si-AGT groups (all $P>0.05$). Compared with the blank, empty plasmid and miR-29a inhibitors + si-AGT groups, the expression levels of VEGF, HGF, ANG and AngII significantly decreased in the miR-29a mimics, miR-29a mimics + si-AGT and si-AGT groups (all $P<0.05$). The expression levels of VEGF, HGF, ANG and AngII in the miR-29a mimics + si-AGT group were lower than those in the miR-29a mimics group; the expression levels of VEGF, HGF, ANG and AngII in the miR-29a inhibitors group were higher than those in the miR-29a inhibitors + si-AGT group (all $P<0.05$) (**Figure 8**). These results indicated

that the miR-29a mimics and inhibitors could, respectively, inhibit or promote the expression levels of VEGF, HGF, ANG and AngII, and these effects could be reversed by silencing AGT.

**Discussion**

Currently, it is generally believed that retinal neovascularization is one of the leading factors of ROP [21]. Angiogenesis can be caused by the up-regulation of vascular growth factors at the onset of ischemia or hypoxia [22]. Many angiogenesis factors, such as VEGF, ANG and HGF, have been found to be connected to ROP [5-7]. In this paper, the targeting effect of miR-29a on the AGT gene was investigated in hopes of determining the mechanism of targeted therapy in treating ROP.

In this study, ROP mouse models were constructed by oxygen induction. Compared with normal mice, the miR-29a expression decreased, and the mRNA and protein expression levels of AGT increased in ROP mice. It was speculated here that the down-regulation of miR-29a led to the increase in AGT, which accelerates the formation of retinal neovascularization. It was reported that an independent renin angiotensin aldosterone system (RAAS) exists in ocular tissues, and this RAAS participated in the pathophysiological processes of ROP and other proliferative eye diseases [23]. The AngII activation signal is a key mediator that promotes cell growth and vascular proliferation, and it might be involved in the development of ROP [24, 25]. In addition, it was found in this study that AGT was negatively associated with miR-29a expression in 293T cells, and miR-29a could negatively regulate transcription of the AGT gene, although the intrinsic mechanism remains unknown.

Finally, this study also found that the expression levels of ROP-related factors, such as HGF, VEGF, ANG and AngII, were increased in ROP mice. VEGF is a polypeptide growth factor closely correlated with the proliferation of blood vessels, and it is an important inducing factor in the formation of retinal neovascularization
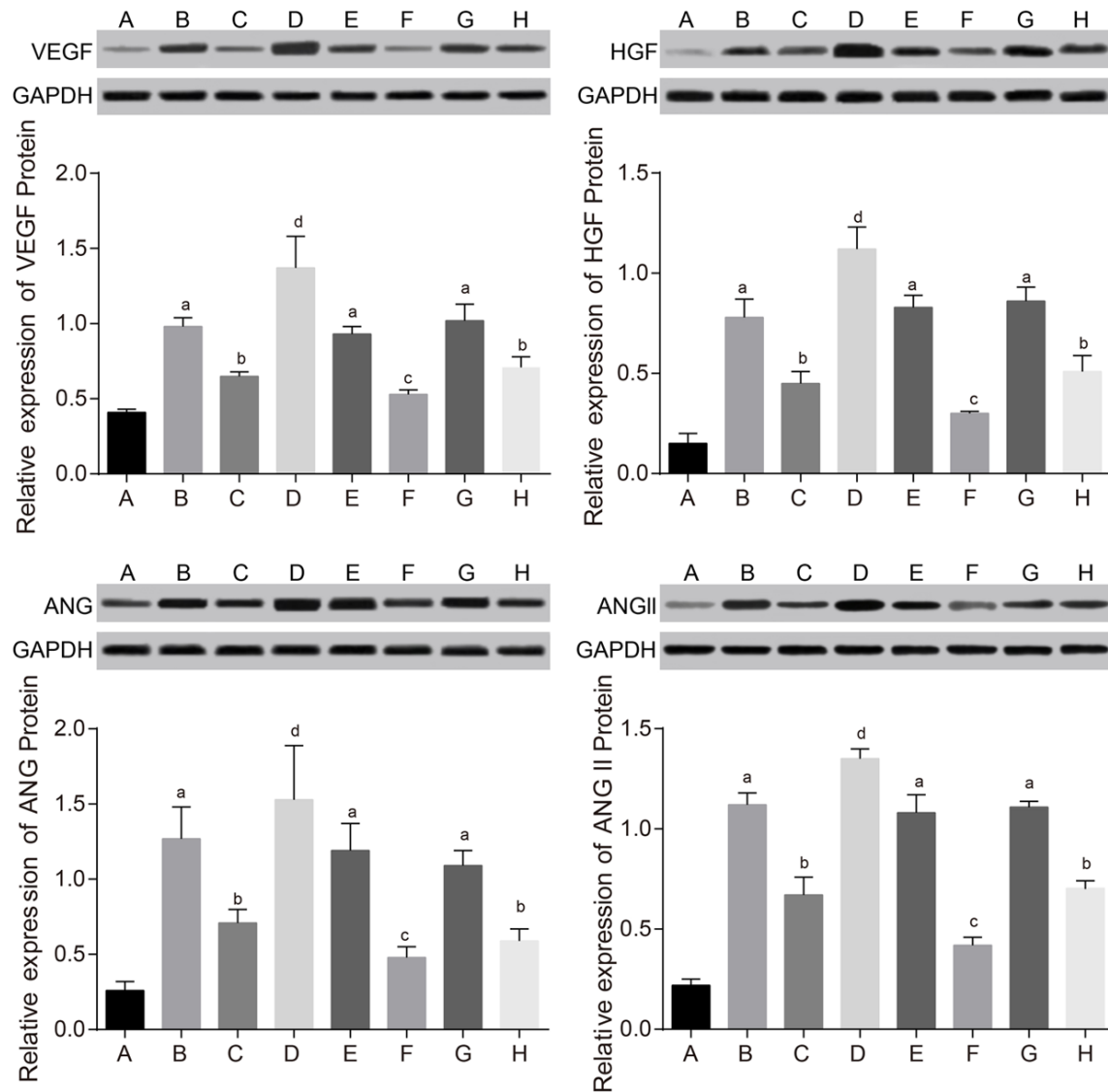
**Figure 8.** The protein expressions levels of VEGF, HGF, ANG and AngII in eight groups. Notes: A. normal control group; B. blank group; C. miR-29a mimics group; D. miR-29a inhibitors group; E. empty plasmid group; F. miR-29a mimics + si-AGT group; G. miR-29a inhibitors + si-AGT group; H. si-AGT group; lowercase letters indicate *P*<0.05, compared with the normal control group: different letters indicate *P*<0.05 comparing two groups, while the same letters indicate *P*>0.05 comparing two groups; VEGF = vascular endothelial growth factor; HGF = hepatocyte growth factor; ANG = angiotensin; AngII = angiotensin II; AGT = angiotensinogen.

[26]. In hypoxic and ischemic retinopathy, VEGF was up-regulated, and it participated in damage to the blood-retinal barrier [27, 28]. HGF is a pleiotropic growth factor of mesenchymal origin, and it has strong functions of promoting cell division, tissue formation, epithelial cell migration, cell invasion and angiogenesis [29]. By stimulating both the growth and migration of endothelial cells, HGF is a strong inducer of angiogenesis that influences vascularization by

mediating or modulating interactions between endothelial cells and pericytes, modulating extracellular matrix production and thereby contributing to retinal detachment [30, 31]. It was shown that HGF is involved in the formation of retinal neovascularization during proliferative diabetic retinopathy (DR) [30]. AngII interacts with specific growth factors, such as VEGF, to influence retinal angiogenesis in the occurrence and development of proliferative

retinopathy [18, 19]. It has been found that, in animal models of retinopathy, AngII was up-regulated, but AngI was only slightly increased, causing an imbalance in the ratio of AngII to AngI, which might contribute to explaining the increase in AngII expression [32, 33]. In this study, the ROP mice also showed vascular derangements, tortuosity, and increases in vascular density and retinal neovascularization. Therefore, retinal neovascularization and related pathological changes could be promoted by the interaction of various vascular growth factors.

In summary, our findings provided evidence that miR-29a could inhibit retinal neovascularization to prevent the development and progression of ROP by down-regulating AGT. Our study could provide some insight for the clinical treatment of ROP. However, there are some limitations to this study, including the lack of clinical data and non-comprehensive mechanisms in understanding the role of miR-29a in ROP, which should be explored in future studies.

## Disclosure of conflict of interest

None.

Address correspondence to: Dr. Lian-Hong Pi, Department of Ophthalmology, Children's Hospital, Chongqing Medical University, No. 136 Zhongshan Er Road, Chongqing 400016, P. R. China. Tel: +86-23-63622874; Fax: +86-23-63622874; E-mail: chongqingplh@126.com

## References

[1] Uhumwangho O and Israel-Aina Y. Awareness and screening for retinopathy of prematurity among paediatricians in Nigeria. J West Afr Coll Surg 2013; 3: 33-45.

[2] Chan JJ, Lam CP, Kwok MK, Wong RL, Lee GK, Lau WW and Yam JC. Risk of recurrence of retinopathy of prematurity after initial intravitreal ranibizumab therapy. Sci Rep 2016; 6: 27082.

[3] Bharwani SK and Dhanireddy R. Systemic fungal infection is associated with the develop-ment of retinopathy of prematurity in very low birth weight infants: a meta-review. J Perinatol 2008; 28: 61-66.

[4] Stahl A and Gopel W. Screening and treatment in retinopathy of prematurity. Dtsch Arztebl Int 2015; 112: 730-735.

[5] Eldweik L and Mantagos IS. Role of VEGF inhibition in the treatment of retinopathy of prematurity. Semin Ophthalmol 2016; 31: 163-168.

[6] Zhang S, Zhai G, Shi W, Wang Y, Zhu L, Dai Y and Chen C. Pigment epithelium-derived factor inhibits oxygen-induced retinal neovascularization in a murine model. Fetal Pediatr Pathol 2016; 35: 173-185.

[7] Jo H, Jung SH, Yim HB, Lee SJ and Kang KD. The effect of baicalin in a mouse model of retinopathy of prematurity. BMB Rep 2015; 48: 271-276.

[8] Cerman E, Ozarslan Ozcan D, Celiker H, Eraslan M, Sahin O and Kazokoglu H. Late clinical characteristics of infants with retinopathy of prematurity and treated with cryotherapy. Int J Ophthalmol 2016; 9: 567-571.

[9] Kara C, Petricli IS, Hekimoglu E, Akil H and Beyazyildiz O. Treatment success of laser therapy for retinopathy of prematurity in referred and non-referred patients. Arq Bras Oftalmol 2016; 79: 96-99.

[10] Di Y, Zhang Y, Yang H, Wang A and Chen X. The mechanism of CCN1-enhanced retinal neovascularization in oxygen-induced retinopathy through PI3K/Akt-VEGF signaling pathway. Drug Des Devel Ther 2015; 9: 2463-2473.

[11] Kovacs B, Lumayag S, Cowan C and Xu S. MicroRNAs in early diabetic retinopathy in streptozotocin-induced diabetic rats. Invest Ophthalmol Vis Sci 2011; 52: 4402-4409.

[12] Monteleone K, Selvaggi C, Cacciotti G, Falasca F, Mezzaroma I, D'Ettorre G, Turriziani O, Vullo V, Antonelli G and Scagnolari C. MicroRNA-29 family expression and its relation to antiviral immune response and viro-immunological markers in HIV-1-infected patients. BMC Infect Dis 2015; 15: 51.

[13] Hirota K, Keino H, Inoue M, Ishida H and Hirakata A. Comparisons of microRNA expression profiles in vitreous humor between eyes with macular hole and eyes with proliferative diabetic retinopathy. Graefes Arch Clin Exp Ophthalmol 2015; 253: 335-342.

[14] Zhuo JL, Kobori H, Li XC, Satou R, Katsurada A and Navar LG. Augmentation of angiotensinogen expression in the proximal tubule by intracellular angiotensin II via AT1a/MAPK/NF-small ka, CyrillicB signaling pathways. Am J Physiol Renal Physiol 2016; 310: F1103-1112.

[15] Wu SJ, Soulez M, Yang YH, Chu CS, Shih SC, Hebert MJ, Kuo MC and Hsieh YJ. Local aug-

mented angiotensinogen secreted from apoptotic vascular endothelial cells is a vital mediator of vascular remodelling. PLoS One 2015; 10: e0132583.

[16] Singh A, Vitko J, Re RN and Cook JL. Intracellular enhanced cyan fluorescent protein/angiotensin II does not modify angiotensinogen accumulation in transgenic mice. Ochsner J 2013; 13: 37-41.

[17] Wu C, Xu Y, Lu H, Howatt DA, Balakrishnan A, Moorleghen JJ, Vander Kooi CW, Cassis LA, Wang JA and Daugherty A. Cys18-Cys137 disulfide bond in mouse angiotensinogen does not affect AngII-dependent functions in vivo. Hypertension 2015; 65: 800-805.

[18] Carbajo-Lozoya J, Lutz S, Feng Y, Kroll J, Hammes HP and Wieland T. Angiotensin II modulates VEGF-driven angiogenesis by opposing effects of type 1 and type 2 receptor stimulation in the microvascular endothelium. Cell Signal 2012; 24: 1261-1269.

[19] Nadal JA, Scicli GM, Carbini LA and Scicli AG. Angiotensin II stimulates migration of retinal microvascular pericytes: involvement of TGF-beta and PDGF-BB. Am J Physiol Heart Circ Physiol 2002; 282: H739-748.

[20] Feng F, Cheng Y and Liu QH. Bevacizumab treatment reduces retinal neovascularization in a mouse model of retinopathy of prematurity. Int J Ophthalmol 2014; 7: 608-613.

[21] Di Y, Zhang Y, Nie Q and Chen X. CCN1/Cyr61-PI3K/AKT signaling promotes retinal neovascularization in oxygen-induced retinopathy. Int J Mol Med 2015; 36: 1507-1518.

[22] Heidary G, Vanderveen D and Smith LE. Retinopathy of prematurity: current concepts in molecular pathogenesis. Semin Ophthalmol 2009; 24: 77-81.

[23] Wilkinson-Berka JL, Agrotis A and Deliyanti D. The retinal renin-angiotensin system: roles of angiotensin II and aldosterone. Peptides 2012; 36: 142-150.

[24] Ha YM, Nam JO and Kang YJ. Pitavastatin regulates Ang II induced proliferation and migration via IGFBP-5 in VSMC. Korean J Physiol Pharmacol 2015; 19: 499-506.

[25] Wilkinson-Berka JL, Rana I, Armani R and Agrotis A. Reactive oxygen species, Nox and angiotensin II in angiogenesis: implications for retinopathy. Clin Sci (Lond) 2013; 124: 597-615.

[26] Fleck BW and McIntosh N. Pathogenesis of retinopathy of prematurity and possible preventive strategies. Early Hum Dev 2008; 84: 83-88.

[27] Shi RZ, Wang JC, Huang SH, Wang XJ and Li QP. Angiotensin II induces vascular endothelial growth factor synthesis in mesenchymal stem cells. Exp Cell Res 2009; 315: 10-15.

[28] Skondra D, Noda K, Almulki L, Tayyari F, Frimmel S, Nakazawa T, Kim IK, Zandi S, Thomas KL, Miller JW, Gragoudas ES and Hafezi-Moghadam A. Characterization of azurocidin as a permeability factor in the retina: involvement in VEGF-induced and early diabetic blood-retinal barrier breakdown. Invest Ophthalmol Vis Sci 2008; 49: 726-731.

[29] Jiang WG. Hepatocyte growth factor and the hepatocyte growth factor receptor signalling complex as targets in cancer therapies. Curr Oncol 2007; 14: 66-69.

[30] Simo R, Carrasco E, Garcia-Ramirez M and Hernandez C. Angiogenic and antiangiogenic factors in proliferative diabetic retinopathy. Curr Diabetes Rev 2006; 2: 71-98.

[31] Lashkari K, Hirose T, Yazdany J, McMeel JW, Kazlauskas A and Rahimi N. Vascular endothelial growth factor and hepatocyte growth factor levels are differentially elevated in patients with advanced retinopathy of prematurity. Am J Pathol 2000; 156: 1337-1344.

[32] Sato T, Shima C and Kusaka S. Vitreous levels of angiopoietin-1 and angiopoietin-2 in eyes with retinopathy of prematurity. Am J Ophthalmol 2011; 151: 353-357, e351.

[33] Davis B, Dei Cas A, Long DA, White KE, Hayward A, Ku CH, Woolf AS, Bilous R, Viberti G and Gnudi L. Podocyte-specific expression of angiopoietin-2 causes proteinuria and apoptosis of glomerular endothelia. J Am Soc Nephrol 2007; 18: 2320-2329.